

A

Atmospheric Turbulence



Warren E. Heilman¹, Craig B. Clements², Shiyuan Zhong³, Kenneth L. Clark⁴, and Xindi Bian¹

¹USDA Forest Service, Northern Research Station, Lansing, MI, USA

²Department of Meteorology and Climate Science, San José State University, San José, CA, USA

³Department of Geography, Environment, and Spatial Sciences, Michigan State University, East Lansing, MI, USA

⁴USDA Forest Service, Northern Research Station, New Lisbon, NJ, USA

Synonyms

[Instability](#); [Turbulent eddies](#); [Vortices](#); [Wind and temperature fluctuations](#); [Wind gusts](#)

Definition

Atmospheric turbulence is irregular fluctuations occurring in atmospheric air flow. These fluctuations are random and continuously changing and are superimposed on the mean motion of the air (American Meteorological Society 2018).

Introduction

It has long been established that the behavior of wildland fires and the dispersion of smoke during wildland fire events are influenced by ambient and fire-induced winds (Crosby 1949; Byram and Nelson 1951; Byram 1954; Gifford 1957; Rothermel 1972; Raupach 1990; Beer 1991). Fundamentally, ambient and fire-induced winds affect the horizontal and vertical convective flux of heat in the fire environment and the ability of spreading fires to transfer heat convectively to potential fuels (Rothermel 1972). The transport of firebrands away from active burning locations and the opportunity for spotting ignitions are also governed by the ambient and fire-induced wind fields within and near the fire environment (Koo et al. 2010). Finally, ambient and fire-induced circulations in the lower atmospheric boundary layer (ABL), the lowest layer of the atmosphere, act to disperse emissions away from fires, which often results in the subsequent long-range transport of smoke plumes by winds in the ABL and above to locations far downwind of the burning location (Liu et al. 2009; Heilman et al. 2014).

As described in Stull (1988), the wind field at any location, regardless of whether a fire is present or not, can be partitioned into three components: the mean wind, waves, and turbulence. The rapid transport of heat, moisture, momentum, pollutants, and other scalars is accomplished via the mean wind, with horizontal mean wind speeds usually much larger than vertical mean wind speeds in the ABL. Waves in the wind field

are often generated by shears in the mean wind and by wind flow over obstacles and are very effective at transporting momentum and energy. The relatively high-frequency fluctuations that can occur in the wind field, particularly in the ABL, are characterized as turbulence or wind gusts superimposed on the mean wind. Turbulence is often visualized as eddies or swirls (i.e., vortices) of atmospheric motion of many different sizes superimposed on each other (Stull 1988).

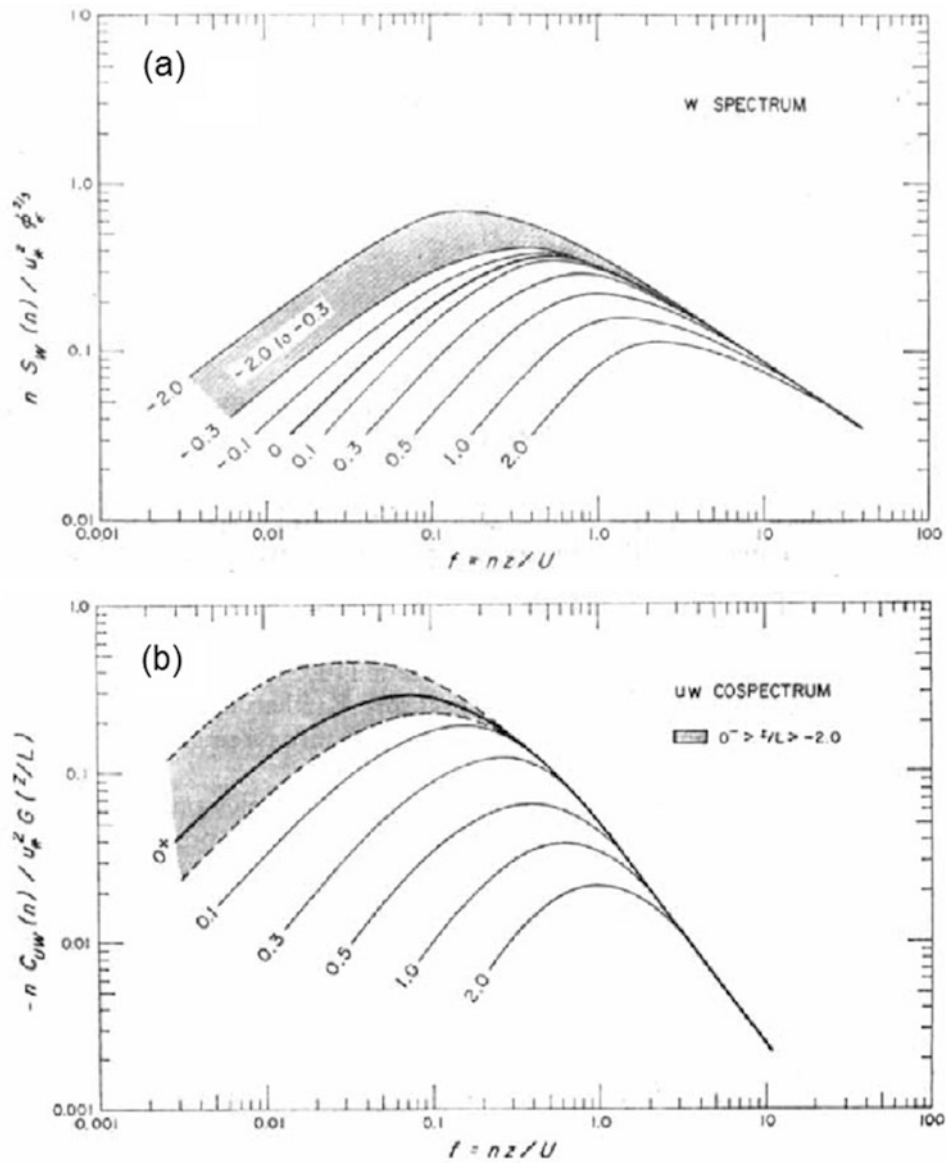
Ambient turbulence (i.e., no fire-induced turbulence) in the daytime ABL is generated in part by buoyancy associated with solar heating of the surface, which leads to rising warmer air within thermal plumes and compensating sinking motion and horizontal convergent and divergent flows over areas adjacent to and outside the thermal plumes (Stull 1988; Wyngaard 1992). Ambient turbulence in the ABL is also generated by wind shears associated with frictional drag imposed on air as it flows over the ground. The presence of obstacles like forest canopies and structures can deflect atmospheric flow near the surface and generate additional turbulent eddies adjacent to and downwind of the obstacles (Raupach and Thom 1981; Finnigan 2000; Roth 2000). The turbulent eddies generated by these processes can range in size from $\sim 10^{-1}$ to 10^3 m, with most of the energy contained in the large eddies. Large eddies are continually broken down in size to smaller and less energetic eddies via the energy cascade process and then eventually dissipated (Batchelor 1950).

Many observation- and modeling-based studies have been carried out to investigate the properties of ambient atmospheric turbulence regimes that characterize the ABL, and they have laid the foundation for subsequent studies focused on how wildland fires affect ABL turbulence (i.e., the combination of fire-induced and ambient turbulence) and its feedback on fire behavior and smoke dispersion. The following sections provide an overview of the key findings from these studies.

Ambient Atmospheric Turbulence Overview

The properties of atmospheric turbulence have been studied extensively over the past 100+ years. Counihan (1975) provided a comprehensive summary of some of the early atmospheric turbulence studies that set the stage for more recent observational and modeling studies relevant to turbulence effects on wildland fires. Included in the summary were the very early studies of Rawson (1913), Shaw (1914), and Richardson (1920), who noted that atmospheric motions can be turbulent with turbulence intensity usually decreasing with height; that turbulence changes its character when obstacles are encountered; and that the kinetic energy of turbulent eddies is extracted from the mean wind, respectively. Shortly after these studies, Goldie (1925) and Best (1935) reported that turbulent eddies near the ground surface tend to break down into smaller sizes, and the eddy velocities in the longitudinal, lateral, and vertical directions tend to be different, an indication that turbulence in the ABL is typically anisotropic. The concept of turbulence anisotropy was further confirmed in the subsequent studies of Panofsky and McCormick (1954) and Deacon (1955). The landmark studies of Taylor (1938) and Kolmogorov (1941) provided new insight at that time into how the energy of turbulent eddies typically varies with eddy size. They showed through theoretical analyses that (1) large-scale eddies (length scale $\sim 10^3$ – 10^1 m; Wyngaard 1992) associated with low-frequency (10^{-3} – 10^{-1} Hz) fluctuations in the wind field contain most of the energy in the turbulence field, (2) within the mid-frequency range ($\sim 10^{-1}$ – 10^1 Hz) of wind fluctuations (also called the inertial subrange; length scale $\sim 10^1$ – 10^{-1} m; Wyngaard 1992), turbulence energy tends to decrease as the frequency increases according to Kolmogorov's $-5/3$ power law (e.g. see Fig. 1a), and (3) turbulence energy is dissipated at the high-frequency (10^3 Hz) portion of the turbulence spectrum (length scale $\sim 10^{-3}$ m; Wyngaard 1992).

More recent turbulence studies conducted during the last half of the twentieth century included



Atmospheric Turbulence, Fig. 1 Generalized frequency-weighted (a) vertical velocity (w) spectra and (b) momentum flux (uw , Reynolds stress) cospectra as a function of normalized frequency (f) for typical atmospheric surface layers under different stability conditions as quantified by z/L values ranging from $+2.0$ (stable) to -2.0 (unstable), where z is the height AGL

and L is the Obukhov length. (From Kaimal et al. 1972). Stippling indicates absence of any well-defined trend with z/L . The slopes of the spectra (a) and cospectra (b) curves in the inertial subrange ($f > 1.0$) approach $-2/3$ and $-4/3$, respectively, corresponding to slopes of $-5/3$ and $-7/3$ for non-frequency-weighted spectra and cospectra

numerous field experiments to measure the properties of ambient ABL turbulence regimes and evaluate earlier theoretical results. The Wangara Experiment conducted in New South Wales, Australia, in 1967 (Clarke et al. 1971), and the Kansas

Experiment conducted in southwestern Kansas in 1968 (Haugen et al. 1971; Businger et al. 1971) provided two of the first comprehensive and foundational datasets on ambient ABL turbulence over flat uniform surfaces.

Data from the Wangara Experiment were used as the basis for recommending the value of 0.40–0.41 for the von Karman constant, a constant used in calculating turbulent momentum fluxes in the surface layer from observed vertical wind profiles (Dyer and Hicks 1970; Hicks 1976; Hess et al. 1981; Stull 1988). Data from the Kansas Experiment were used for assessments of typical turbulent kinetic energy (TKE; defined as one-half of the sum of the horizontal and vertical velocity variances) budgets and turbulence spectra/cospectra in the ABL. For example, Wyngaard and Coté (1971) investigated how TKE budgets differ under stable and unstable atmospheric conditions. They found that under unstable ambient atmospheric conditions, typical of daytime ABLs present during many wildland fire events, the production of turbulence energy via buoyancy and wind shear, the viscous dissipation of turbulence energy, and the turbulent transport of turbulence energy are all significant contributors to the evolution of turbulence regimes. However, as daytime instability increases, buoyancy eventually tends to become the dominant factor in generating turbulence. Kaimal et al. (1972) investigated the spectral characteristics of the turbulent circulations and temperatures under different atmospheric stability conditions at the Kansas experimental site and compared those spectral characteristics with the results from similar studies conducted in the 1960s (e.g., Lumley and Panofsky 1964; Berman 1965; Busch and Panofsky 1968). They found that while turbulence in general is anisotropic in the ABL, turbulence associated with high-frequency wind fluctuations tends to be isotropic. They also found that in the inertial subrange, turbulence energy spectra associated with horizontal and vertical wind fluctuations decrease as the frequency of the fluctuations increases according to the Kolmogorov (1941) $-5/3$ power law (Fig. 1a). For the cospectra of the vertical turbulent fluxes of heat and momentum, they found a more rapid inertial subrange decrease as frequency increases, following a $-7/3$ power law (Fig. 1b).

Recognizing that forest and other vegetation canopies have an impact on ambient atmospheric turbulence regimes that develop under stable and

unstable conditions, many investigators in the mid- to late 1900s and early 2000s focused their attention on the theoretical aspects of turbulence within and above canopies and conducting experiments similar to the Kansas experiment but in environments with forest overstory vegetation. These studies, while not focused on ambient turbulence regimes during wildland fire events, are highly relevant given that many wildland fires occur in forested environments.

Wilson and Shaw (1977) developed a one-dimensional turbulence closure model applicable for investigating flow through vegetation canopies and used the model to show that the production of TKE via wind shear and the obstruction of wind flow by vegetation elements (wake effects) tend to be at a maximum at or near the canopy top and just below the canopy top, respectively. Raupach and Thom (1981) in their theoretical description of turbulence regimes within and above plant canopies noted that plant canopies interact with the air flow within and above vegetation layers, resulting in the turbulent flux of heat and momentum through the canopy-atmosphere interface and through the vegetation layer. They also noted that vegetation canopies can generate turbulence through wake effects, similar to the findings of Wilson and Shaw (1977), thereby converting mean kinetic energy of air flow into TKE. Finnigan (2000) drew upon the theoretical work of Wilson and Shaw (1977) and Raupach and Thom (1981) and other canopy studies and provided a summary of the key properties of turbulence regimes within vegetation layers. In that summary, it was noted that turbulent circulations drive the exchange of heat, moisture, and other scalars between the vegetation layer and the atmosphere and that turbulent fluxes of scalars between vegetation layers and the atmosphere are dominated by large coherent eddies that sweep air from aloft into the vegetation layers. This is the typical ambient turbulent flux environment that serves as the backdrop for turbulent fluxes of heat, moisture, and momentum induced by wildland fires occurring in forested areas.

Examples of observational studies of ambient turbulence regimes within and above vege-

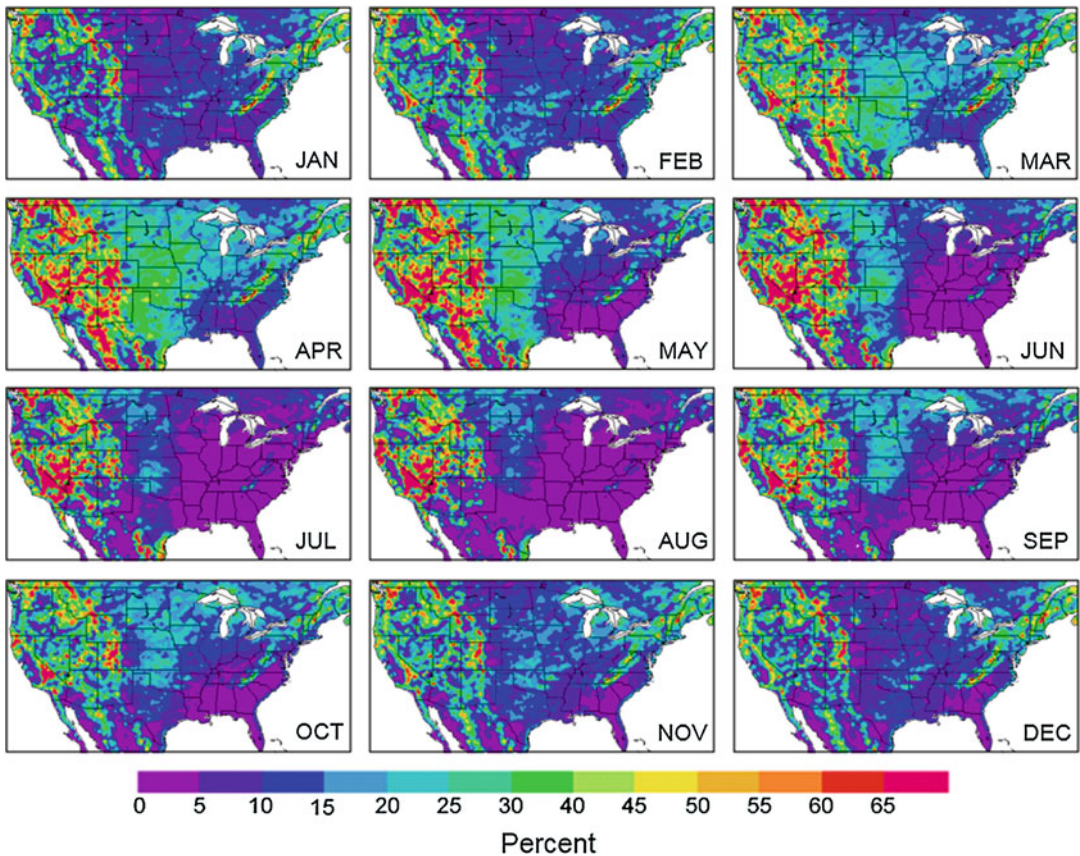
tation canopies include the studies of Shaw et al. (1974, 1988), Baldocchi and Meyers (1988), Amiro (1990), Meyers and Baldocchi (1991), and Vickers and Thomas (2013), plus the many turbulence and energy exchange studies associated with the Ameriflux (<http://ameriflux.lbl.gov/>) and Fluxnet (<https://fluxnet.fluxdata.org/>) programs. These studies provided observational evidence and confirmation for many of the theoretical findings in earlier studies and critical insight into the dynamics of atmospheric turbulence within vegetation layers. Highlights of the results from these studies indicate that (1) turbulence spectra above forest canopies tend to follow the Kolmogorov $-5/3$ power law in the inertial subrange, (2) the slopes of the power spectra measured within forest canopies are more negative than those observed in the typical surface boundary layer with no forest canopy present, (3) in the bottom portions of forest canopies, horizontal velocity component spectra tend to decrease more rapidly with increasing frequency in the inertial subrange than vertical velocity spectra, (4) turbulent heat and momentum flux cospectra within forest vegetation layers often exhibit slope values close to -1 in the inertial subrange, (5) turbulence spectra within forest canopies tend to peak at higher frequencies than the spectra measured in the subcanopy trunkspace and above the canopy, (6) turbulence above forest canopies associated with high-frequency velocity fluctuations tends to be isotropic, (7) denser canopies tend to inhibit vertical turbulent momentum fluxes within forest vegetation layers, (8) TKE is usually at a maximum at or just above the canopy top, but the relative intensity of turbulence (velocity standard deviation divided by mean wind speed) tends to be at a maximum at mid-canopy levels, (9) thermal stability or buoyancy has a stronger influence on turbulence within vegetation layers than leaf density, (10) wake-generated turbulence can exceed shear-generated turbulence at all levels within forest vegetation layers except near the canopy top, and (11) beneath tree crowns, turbulent transport tends to be the dominant process in TKE evolution, with shear-generated turbulence energy above the canopy top transported downward into the subcanopy layers by turbulence.

Atmospheric Turbulence and Wildland Fires

The behavior of wildland fires is often transient, due to the highly variable winds that can occur in their vicinity. The variability in wind speed and direction near a spreading fire is associated with fire-atmosphere interactions that induce turbulent circulations surrounding the fire and ambient turbulent circulations that are manifestations of eddies in the ABL (Sun et al. 2009; Forthofer and Goodrick 2011). Numerous observational and modeling studies over the last three decades have examined the relationships between wildland fires and ambient or fire-induced turbulence. This section provides a summary of the key results from these studies and an overview of the current state of knowledge regarding the interactions of wildland fires and turbulence.

Observational Studies

Few observational studies have been carried out to examine the association of wildland fire events strictly with ambient atmospheric turbulence. Heilman and Bian (2010) examined the association of wildfires in the north central and northeastern USA with substantial near-surface ambient turbulence. They found that relatively large wildfires in this region of the USA (typically during the spring and autumn seasons) often occur when ambient near-surface TKE values exceed $3 \text{ m}^2 \text{ s}^{-2}$ (a threshold indicative of highly turbulent conditions (Stull 1988); see Fig. 2), at the same time lower atmospheric conditions are relatively dry and unstable, as quantified by the well-known Haines fire-weather index (HI; Haines 1988). A new fire-weather index based on a simple product of TKE and the HI (HITKE) was evaluated by Heilman and Bian (2010) for wildfires in the north central and northeastern USA and was found to be a reasonable indicator of the conduciveness of the ambient atmosphere to extreme fire occurrence (HITKE $>15 \text{ m}^2 \text{ s}^{-2}$). Although assessments of TKE levels during wildfires in other regions of the USA have not been completed yet, it is hypothesized that large and extreme wildfires in these regions also tend to occur when near-



Atmospheric Turbulence, Fig. 2 Average percentage of days each month that have daily maximum turbulent kinetic energy values near the surface greater than $3 \text{ m}^2 \text{ s}^{-2}$ based on data from the North American Re-

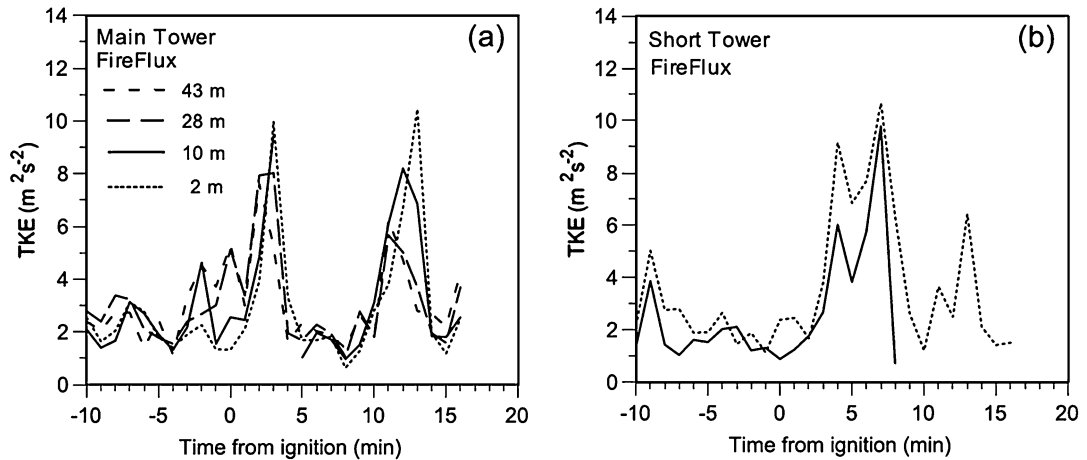
gional Reanalysis (Mesinger et al. 2006) for the 1979–2008 period. (From Heilman and Bian 2013; ©American Meteorological Society; Used with permission)

surface atmospheric turbulence is substantial. For example, over the western complex-terrain regions of the USA where large wildfires are common, occurrences of high TKE values near the surface are relatively frequent (Fig. 2) (Heilman and Bian 2013). The interaction of ambient turbulent eddies with wildland fires in areas of complex terrain can lead to erratic fire behavior, such as that associated with fire channeling, a phenomenon where rapid fire spread occurs in a direction transverse to the mean ambient wind (Byron-Scott 1990; Sharples et al. 2012).

Investigations of wildland fire effects on ambient turbulence regimes have been more common. Early efforts to analyze how wildland fires can alter typical ambient turbulence regimes in

the ABL include the studies of Graham (1955), Byram and Martin (1970), Church et al. (1980), Emori and Saito (1982), Haines (1982), Haines and Smith (1983, 1987, 1992), Church and Snow (1985), McRae and Flannigan (1990), and Banta et al. (1992). These studies provided observational evidence of the formation of horizontally and vertically oriented turbulent vortices (i.e., coherent eddies) in the vicinity of wildland fires or heat sources similar to wildland fires. The formation of unburned tree-crown streets in the aftermath of some wildland fires in forested environments has been attributed to fire-generated horizontally oriented turbulence vortices, also known as horizontal roll vortices, by Haines (1982).

With the development of more sophisticated monitoring technology for measuring fire-fuel-



Atmospheric Turbulence, Fig. 3 Time series of observed turbulent kinetic energy ($\text{m}^2 \text{s}^{-2}$) at different heights on the (a) 43 m main tower and (b) 10 m short tower during the FireFlux I grass fire experiment con-

ducted on 23 February 2006 at the University of Houston's Coastal Center. (From Clements et al. 2008). Towers were located in the interior of the burn plot

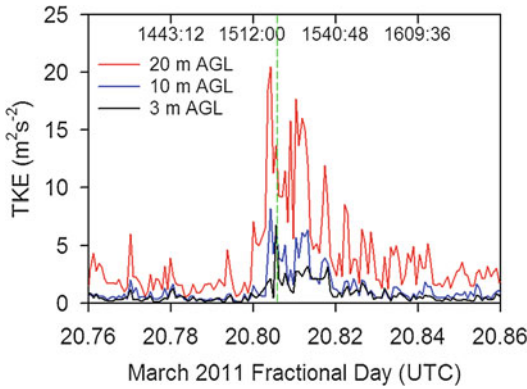
atmosphere interactions in the late twentieth and early twenty-first centuries, significant advances were made in improving our understanding of how fire-induced turbulence regimes differ from the regimes that characterize a typical ABL and how they interact with ambient turbulence regimes to affect fire behavior and smoke dispersion. While turbulence-related measurements were fairly limited in the well-known 1997 International Crown Fire Modeling Experiment (ICFME; Alexander et al. 1998), the 1998 Wildfire Experiment (WiFE; Radke et al. 2000), and the 1999 FROSTFIRE experiment (Coen et al. 2004), more comprehensive in situ measurements of turbulence regimes within and near wildland fire fronts were carried out in the early 2000s. These experiments included both grass fires (e.g., Clements et al. 2007, 2008, 2015, 2016; Clements 2010; Seto and Clements 2011; Charland and Clements 2013; Seto et al. 2013; Clements and Seto 2015; Ottmar et al. 2016) and surface fires beneath forest canopies (e.g., Heilman et al. 2013, 2015, 2017; Strand et al. 2013; Seto et al. 2013, 2014; Ottmar et al. 2016).

Collectively, the aforementioned observational studies suggest wildland fires can lead to turbulent boundary-layer circulations with characteristics substantially different from

those observed under nonfire conditions. First, wildland fires can generate large horizontally oriented turbulent eddies (vortices) with upward and downward turbulent velocities on the order of 10 m s^{-1} or stronger near the surface and near-surface horizontal turbulent velocities 2–3 times larger than ambient horizontal velocities. Turbulent horizontal roll vortices frequently occur immediately in front of and behind fire fronts, with those vortices contributing to flow convergence into the convective plumes situated above and downwind of fire fronts and to downdrafts with near-surface cooling behind the fronts.

Second, typical TKE values above spreading grass-fire fronts ($\sim 10\text{--}20 \text{ m}^2 \text{ s}^{-2}$) greatly exceed the ambient TKE values typically observed in the lower daytime ABL ($\sim 1\text{--}4 \text{ m}^2 \text{ s}^{-2}$), with the height of maximum TKE usually found $\sim 2\text{--}10 \text{ m}$ above ground level (see Fig. 3). For spreading surface fires beneath forest canopies, TKE values above fire fronts also increase substantially from typical daytime TKE values observed within and above forest overstory layers, but maximum increases are usually found above the canopy top instead of closer to the surface as with grass fires (see Fig. 4).

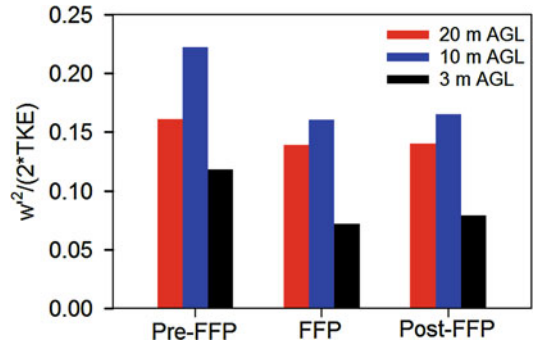
Third, turbulence regimes in the vicinity of spreading surface fires are generally anisotropic,



Atmospheric Turbulence, Fig. 4 Time series of observed 1-min averaged turbulent kinetic energy ($\text{m}^2 \text{s}^{-2}$) at three levels on a 20 m tower during a low-intensity wildland fire experiment conducted on 20 March 2011 in the New Jersey Pine Barrens. (From Heilman et al. 2015). The tower was located in the interior of the burn plot containing pitch pine and mixed oak overstory vegetation ($\sim 15\text{--}18$ m tree heights). Time of fire-front-passage is indicated by green dashed line. Local time (hhmm:ss) is noted below the top axis

meaning there is an unequal distribution of energy among the horizontal and vertical components of TKE. Most of the energy of turbulent eddies found in the vicinity of surface wildland fires is associated with fluctuations in the horizontal turbulent velocity components, which is also the case for ambient turbulent eddies in the ABL. Even within convective plumes immediately above surface fires where buoyancy is substantial and vertical velocity fluctuations are enhanced, turbulence still tends to be anisotropic with the horizontal components of TKE exceeding the vertical component. When forest overstory vegetation is present during surface wildland fire events, turbulence tends to be the most anisotropic near the surface and least anisotropic at mid-canopy levels before (pre-), during, and after (post-) fire front passage (FFP) (see Fig. 5). The anisotropy in turbulence regimes induced by spreading surface fires is most pronounced for large eddy sizes, as is the case for ambient turbulence regimes in the ABL.

Fourth, the production of TKE by vertical wind shear and buoyancy increases significantly during FFP periods. If forest overstory vegetation is present during FFP, the production of



Atmospheric Turbulence, Fig. 5 Observed turbulence anisotropy as quantified by average values of $\overline{w'^2}/(2 \cdot \text{TKE})$, where $\overline{w'^2}$ is the 1-min averaged vertical velocity variance, during 30-min long pre-FFP, FFP, and post-FFP periods at three levels on a 20 m tower during a low-intensity wildland fire experiment conducted on 20 March 2011 in the New Jersey Pine Barrens. (From Heilman et al. 2015). The tower was located in the interior of the burn plot containing pitch pine and mixed oak overstory vegetation ($\sim 15\text{--}18$ m tree heights)

TKE by shear and buoyancy effects may be particularly enhanced in the upper portions of the canopy layer. Vertical diffusion of turbulence energy also tends to increase significantly during FFP periods, especially in the upper portions of the canopy layer if forest overstory vegetation is present. Diffusion contributes to a decrease in turbulence energy at all levels within forest overstory vegetation layers during FFP periods.

Fifth, spreading wildland fires affect the skewness of the daytime horizontal and vertical turbulent velocity distributions that characterize the typical air flow through forest vegetation layers. In particular, vertical velocity distributions that tend to be negatively skewed inside forest vegetation layers (Amiro 1990) become positively skewed during FFP periods. Skewness analyses also suggest that after FFP, vertical velocity distributions can become even more negatively skewed than the negative skewness typically observed in ambient canopy-flow environments. The observed skewness and associated non-Gaussian nature of turbulent circulations in the vicinity of spreading wildland fires through forested areas can make the application of predictive tools that assume Gaussian turbulence

regimes problematic for local smoke dispersion forecasts.

Some of the recent wildland fire observational studies have also examined the spectral characteristics of turbulent circulations that occur in the vicinity of spreading wildland fires. Clements et al. (2008), Seto et al. (2013), and Heilman et al. (2015) revealed in their studies that TKE increases in the vicinity of wildland fires are associated with increases in both horizontal (streamwise) and vertical velocity fluctuations occurring over the $\sim 10^{-3}$ – 10^0 s⁻¹ frequency range (see Figs. 6 and 7). Within the inertial subrange, horizontal and vertical velocity power spectra before and after FFP tend to decrease with increasing frequency according to the Kolmogorov (1941) $-5/3$ power law ($-2/3$ power law for frequency-weighted spectra), similar to what is observed for near-surface velocity spectra in the ambient atmosphere. During FFP periods, however, the decrease in turbulent velocity power spectra values with increasing frequency in the inertial subrange can be much less pronounced, with spectral curve slopes sometimes approaching zero. The shedding of small turbulent eddies from fire fronts has been hypothesized as the reason for the diminished spectral curve slopes in the inertial subrange during FFP periods (Seto et al. 2013).

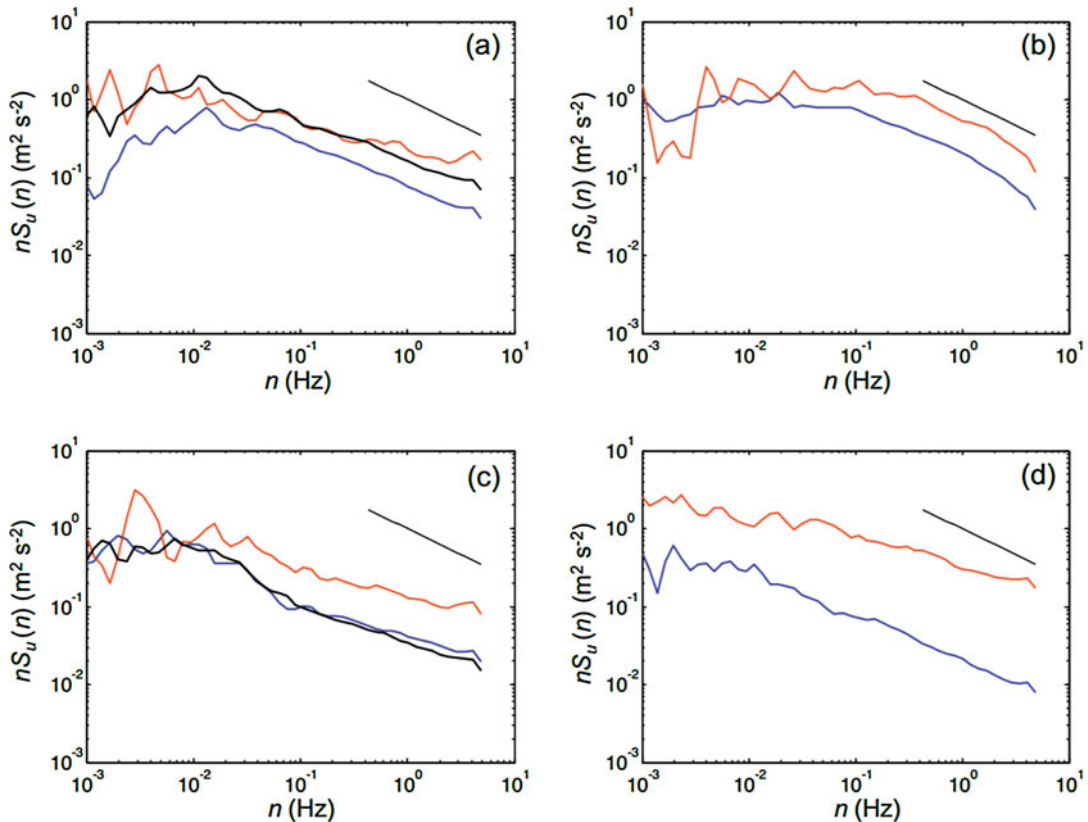
As noted previously, overall turbulence regimes in wildland fire environments are anisotropic. Comparisons of the horizontal and vertical velocity spectra across the range of frequencies governing the horizontal and vertical velocity fluctuations indicate that most of the anisotropy (vertical to horizontal spectra ratios $\ll 1$) that occurs in turbulence regimes before, during, and after FFP can be attributed to large turbulent eddies (low-frequency velocity fluctuations). Spectral analyses from grass-fire experiments show that turbulence associated with small turbulent eddies (high-frequency velocity fluctuations) during the pre-FFP, FFP, and post-FFP periods is fairly isotropic (Seto et al. 2013), with spectra ratios approaching the value of 1.33 as required for isotropic turbulence (Kolmogorov 1941; Lumley and Panofsky 1964). However, similar spectral

analyses from wildland fire experiments conducted in forested environments (Heilman et al. 2015) suggest that turbulence associated with high-frequency velocity fluctuations within forest overstory vegetation layers is somewhat more anisotropic, with spectra ratios at high frequencies approaching a value of 1 or less (see Fig. 8). This is consistent with the findings of Amiro (1990) and Biltoft (2001) related to turbulence isotropy occurrence in near-surface flow with and without a forest canopy present, respectively, under nonfire conditions.

Modeling Studies

Many numerical modeling studies related to fire behavior and fire-atmosphere interactions have been conducted since the early 1990s (Sullivan 2009), with some of them also including assessments of ambient and fire-induced turbulence and their effects on fire behavior and smoke dispersion. Building on some of the pre-1990 observational studies of atmospheric turbulence regimes generated by wildland fires (e.g., Haines 1982; Haines and Smith 1983, 1987), Heilman and Fast (1992) and Heilman (1992, 1994) conducted some of the first boundary-layer modeling studies of wildland-fire-induced turbulence, including turbulent horizontal roll vortex development above fires on flat terrain and on hills. These initial two-dimensional modeling studies showed that (1) the TKE of horizontal roll vortices generated by buoyancy above wildfires can be on the order of 10–100 m² s⁻², depending on fire intensity, (2) the height of maximum TKE tends to decrease as the ambient wind speed increases, and (3) wildfires on the windward, leeward, and crest locations in areas of complex terrain produce very different turbulent horizontal roll vortex structures.

More sophisticated fire-atmosphere interaction modeling efforts followed in the late 1990s and early 2000s (Jenkins et al. 2001). These modeling studies provided further insight into the atmospheric dynamics involved in the generation and evolution of ambient and fire-induced turbulent eddies/vortices during wildland fire events in grass and forested environments, and how turbulence regimes can feed back on fire behavior.



Atmospheric Turbulence, Fig. 6 Frequency-weighted power spectra ($\text{m}^2 \text{s}^{-2}$) of the horizontal (streamwise) wind velocity [$nS_u(n)$] as a function of the natural frequency n (Hz) for (a) an experimental grass fire conducted in a valley (Joseph D. Grant County Park, CA), (b) an experimental grass fire conducted on a slope (Camp Parks Reserve Forces Training Area, CA), (c) a prescribed sub-

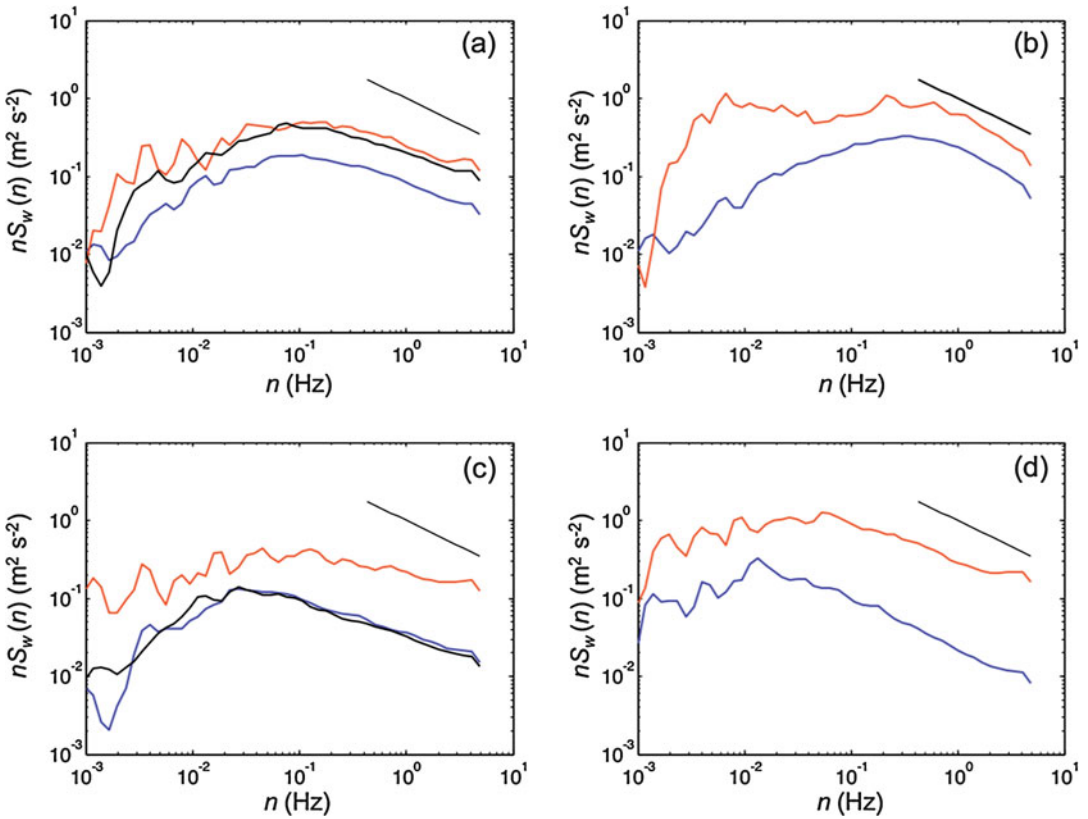
canopy fire (The Nature Conservancy's Calloway Forest, NC), and (d) a slash burn (Hyytiälä, Finland) during pre-FFP (blue), FFP (red), and post-FFP (black) periods. (From Seto et al. 2013). The short line represents the $-2/3$ slope of frequency-weighted velocity spectra in the inertial subrange, as predicted by Kolmogorov (1941)

Some of these modeling efforts and their key findings are described below.

Clark et al. (1996a, b, 2004) used two different coupled fire-atmosphere numerical modeling systems, one utilizing the McArthur fire spread rate formulation (Noble et al. 1980) and the other utilizing the BEHAVE fire-behavior model (Rothermel 1972), to demonstrate that vertically oriented turbulent vortex structures or columns can develop near fire fronts. Furthermore, these vortex structures may lead to significant changes in fire spread rates.

Numerous wildland fire behavior and canopy flow simulations have been carried out with the FIRETEC wildland fire behavior model (Linn et al. 2002) coupled with the HIGRAD atmospheric

transport model (Reisner et al. 2000). Results of the HIGRAD/FIRETEC simulations indicate that (1) large coherent turbulent eddies, which can affect fire spread rates and the occurrence of crown fires, are induced by atmospheric flow through forest canopies (Pimont et al. 2009), (2) unburned tree-crown streets can result from fire-induced horizontally-oriented turbulent vortices (Pimont et al. 2011), reaffirming the unburned tree-crown street formation hypothesis of Haines (1982), (3) vertically oriented turbulent vortices combined with the turbulent buoyant updrafts generated by surface fire lines play a significant role in the transport of firebrands (Koo et al. 2012), (4) turbulent vortices generated by upslope-spreading fire fronts can be transported ahead of the fire



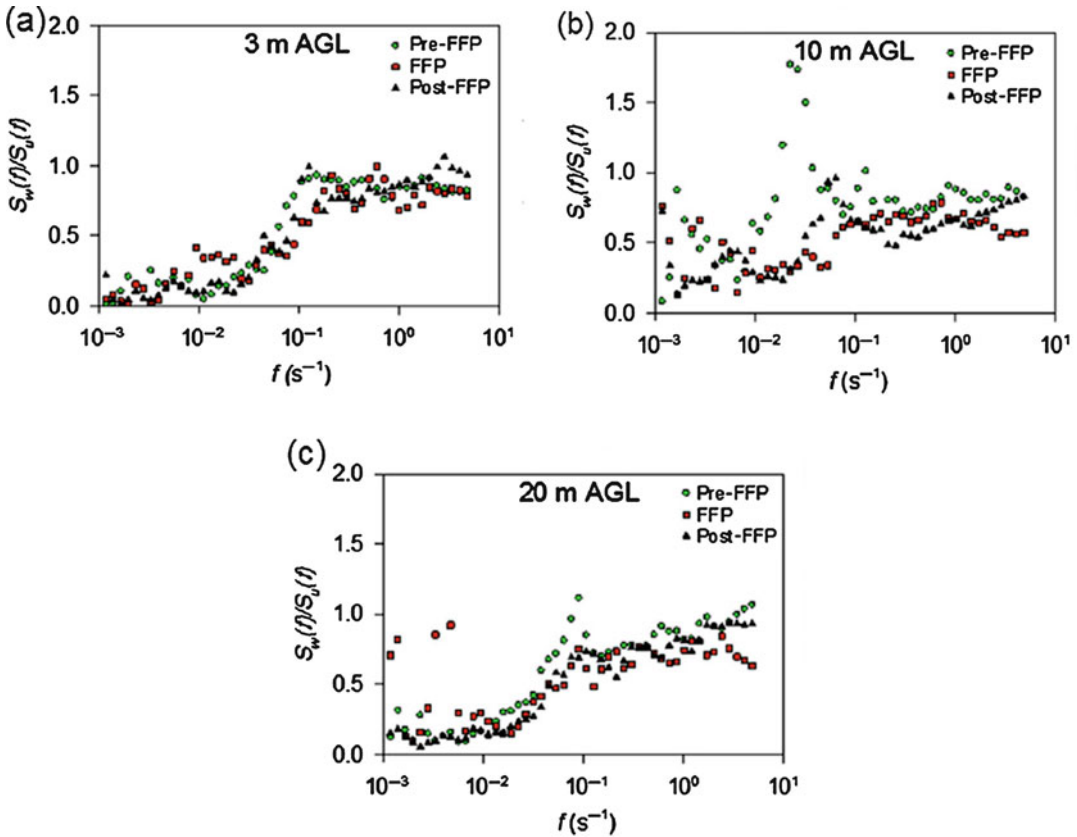
Atmospheric Turbulence, Fig. 7 Same as Fig. 6 except for the frequency-weighted power spectra ($m^2 s^{-2}$) of the vertical wind velocity [$nS_w(n)$]. (From Seto et al. 2013)

fronts and lead to new ignitions at locations relatively far-removed from the fire fronts without any firebrand activity involved (Dupuy and Morvan 2005), (5) buoyancy-induced and horizontally oriented turbulent vortices may develop in the vicinity of fire fronts, leading to regular patterns of up-wash and downwash regions, the latter being associated with penetrating airflow into the fire fronts (Canfield et al. 2014), and (6) forest canopy modifications such as those associated with insect-related defoliation and mortality can lead to changes in the height of maximum TKE from the canopy top to lower heights in the canopy layer, which in turn contribute to changes in potential fire rates of spread over time as tree mortality progresses (Hoffman et al. 2015).

Similar numerical modeling studies of fire-atmosphere interactions have been carried out using the Weather Research and Forecasting (WRF) model (Skamarock et al. 2005) alone

or the wildland fire behavior module WRF-Fire (Coen et al. 2013) integrated into the WRF model. Cunningham et al. (2005) demonstrated with WRF how counter-rotating turbulent vortex pairs aligned with the plume trajectory, transverse vortices generated by wind shear on the upstream face of the plume, and vertically oriented turbulent wake vortices on the downstream side of the plume can develop in response to lower ABL heating by wildland fires. Simpson et al. (2013, 2016) demonstrated with WRF-Fire how fire-induced turbulent updrafts/downdrafts and vertically oriented turbulent eddies/vortices on the flanks of up-slope spreading wildland fires can lead to rapid lateral fire spread near ridge lines.

In addition to the HIGRAD/FIRETEC and WRF/WRF-Fire simulation studies, other studies of ambient and fire-induced turbulence have utilized state-of-the-art modeling systems such

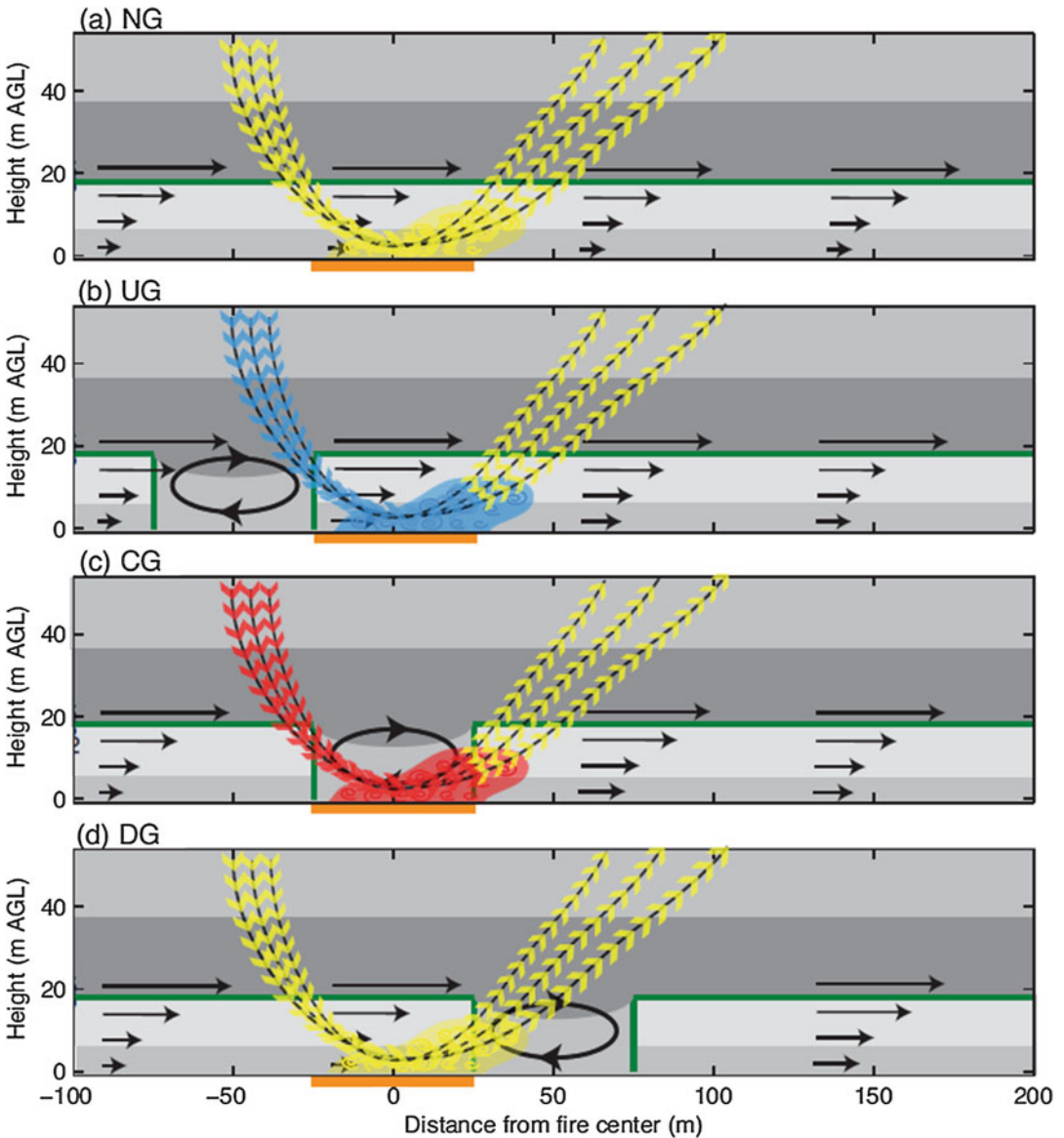


Atmospheric Turbulence, Fig. 8 Ratios of the vertical to horizontal (streamwise) velocity spectra $[S_w(f)/S_u(f)]$ as a function of spectral frequency f (s^{-1}) at (a) 3 m, (b) 10 m, and (c) 20 m levels on a 20 m tower during the pre-FFP, FFP, and post-FFP periods of a low-intensity wildland fire on 20 March 2011 in the New Jersey Pine

Barrens. (From Heilman et al. 2015). The tower was located in the interior of the burn plot containing pitch pine and mixed oak overstory vegetation (~ 15 – 18 m tree heights). Ratio values approaching 1.33 indicate isotropic turbulence

as the University of Utah’s Large-scale Eddy Simulation (UU-LES) model (Zulauf 2001), the Advanced Regional Prediction System (ARPS) (Xue et al. 2000, 2001), the Wildland-Urban-Interface Fire Dynamics Simulator (WFDS) (Mell et al. 2007), and FIRESTAR (Morvan and Dupuy 2004). Sun et al. (2009) used the UU-LES model in their numerical simulations of fire-atmosphere interactions to show that the common occurrence of strong downdrafts behind spreading fire fronts, which can bring high-momentum air from aloft down to the surface, is the result of interactions between fire-induced convective circulations and strong turbulent eddies in the ambient atmosphere. Kiefer et al. (2014, 2015, 2016, 2018) used a version of ARPS

that includes a canopy submodel (ARPS-Canopy; Kiefer et al. 2013) to show that (1) increases in atmospheric TKE above spreading surface fire fronts beneath forest canopies are largest immediately above the canopy top, (2) advection of TKE generated above spreading surface fire fronts can lead to TKE maxima occurring at locations downwind of the fire fronts, (3) both wind shear and buoyancy play a role in TKE production downwind of surface fires when a forest canopy is present, whereas buoyancy is the primary production mechanism in the absence of forest overstory vegetation, (4) the impact of surface fires on boundary-layer integrated vertical turbulent heat fluxes is strongest when no forest overstory vegetation is present, and (5) forest



Atmospheric Turbulence, Fig. 9 Conceptual model of fire-atmosphere interactions with different forest gap configurations: (a) NG – no gap, (b) UG – gap in upstream zone, (c) CG – gap in center zone, (d) gap in downstream zone. (From Kiefer et al. 2016; see https://publications.copernicus.org/for_authors/licence_and_copy_right/license_and_copyright_2007-2017.html for copyright license). Background (i.e., no fire) state indicated with black arrows and grayscale shading: black horizontal arrows indicate the background mean u component of the wind, black oval inside gap represents the gap recirculation zone, and shading indicates background mean TKE

(light (weakest) to dark (strongest)). Fire anomaly fields are depicted with colored arrows and shading: selected fire-line-normal streamlines are indicated with colored arrows, and region of enhanced TKE and turbulent mixing of heat is represented by semi-transparent shading and embedded spirals. The magnitude of the fire anomaly is indicated by the color (blue (weakest) to yellow to red (strongest)). The fire zone is denoted with an orange line, and the perimeter of the forest canopy is indicated with a green line

gaps and their locations with respect to wildland fire lines that may be present have an effect on

turbulent circulations and TKE values upwind and downwind of the fire lines, as depicted in

Fig. 9. Finally, Mueller et al. (2014) and Morvan and Dupuy (2004) were able to show in their WFDS and FIRESTAR simulations, respectively, that (1) ambient turbulence regimes inside forest overstory vegetation layers are characterized by maximum TKE values near the canopy top and positively (negatively) skewed streamwise (vertical) turbulent velocity distributions, and (2) horizontally oriented turbulent vortices just downwind of fire fronts can recirculate hot gases and ignite secondary spot fires if fuel conditions are sufficient.

Cross-References

- ▶ [Convection](#)
- ▶ [Fire Dynamics](#)
- ▶ [Fire Whirls](#)
- ▶ [Fire/Atmosphere Interaction](#)
- ▶ [Firebrands and Embers](#)
- ▶ [Fluid Mechanics](#)
- ▶ [Haines Index](#)
- ▶ [Physics-Based Modeling](#)
- ▶ [Rate of Spread](#)
- ▶ [Smoke Transport](#)
- ▶ [Validation and Verification](#)
- ▶ [Wind](#)

References

- Alexander ME, Stocks BJ, Wutton BM, Flannigan MD, Todd JB, Butler BW, Lanoville RA (1998) The international crown fire modeling experiment: an overview and progress report. Second Symposium on Fire and Forest Meteorology, American Meteorological Society, pp 20–23
- American Meteorological Society (2018) Turbulence. Glossary of meteorology. Available online at <http://glossary.ametsoc.org/wiki/turbulence>
- Amiro BD (1990) Drag coefficients and turbulence spectra within three boreal forest canopies. *Bound-Layer Meteorol* 52:227–246
- Baldocchi DD, Meyers TP (1988) A spectral and lag-correlation analysis of turbulence in a deciduous forest canopy. *Bound-Layer Meteorol* 45:31–58
- Banta RM, Olivier LD, Holloway ET, Kropfli RA, Bartram BW, Cupp RE, Post MJ (1992) Smoke column observations from two forest fires using Doppler lidar and Doppler radar. *J Appl Meteorol* 31:1328–1349
- Batchelor GK (1950) The application of the similarity theory of turbulence to atmospheric diffusion. *Q J R Meteorol Soc* 76:133–146
- Beer T (1991) The interaction of wind and fire. *Bound-Layer Meteorol* 54:287–308
- Berman S (1965) Estimating the longitudinal wind spectrum near the ground. *Q J R Meteorol Soc* 91:302–317
- Best AC (1935) Transfer of heat and momentum in lowest layers of the atmosphere. Geophysical Memorior, Meteorological Office in London, England, no 65
- Biltoft CA (2001) Some thoughts on local isotropy and the 4/3 lateral to longitudinal velocity spectrum ratio. *Bound-Layer Meteorol* 100:393–404
- Busch NE, Panofsky HA (1968) Recent spectra of atmospheric turbulence. *Q J R Meteorol Soc* 94:132–148
- Businger JA, Wyngaard JC, Izumi Y, Bradley EF (1971) Flux-profile relationships in the atmospheric surface layer. *J Atmos Sci* 28:181–189
- Byram, GM (1954) Atmospheric conditions related to blowup fires. Station paper no. 35, USDA Forest Service, Southeastern Forest Experiment Station, Asheville
- Byram GM, Martin RE (1970) The modeling of fire whirlwinds. *For Sci* 16:386–399
- Byram GM, Nelson RM (1951) The possible relation of air turbulence to erratic fire behavior in the southeast. *Fire Control Notes* 12:1–8
- Byron-Scott RAD (1990) The effects of ridge-top and lee-slope fires upon rotor motions in the lee of a steep ridge. *Math Comput Model* 13:103–112
- Canfield JM, Linn RR, Sauer JA, Finney M, Forthofer J (2014) A numerical investigation of the interplay between fireline length, geometry, and rate of spread. *Agric For Meteorol* 189–190:48–59
- Charland AM, Clements CB (2013) Kinematic structure of a wildland fire plume observed by Doppler lidar. *J Geophys Res - Atmos* 118:1–13
- Church CF, Snow JT (1985) Observations of vortices produced by the Météotron. *J Rech Atmosph* 19:455–467
- Church CR, Snow JT, Dessens J (1980) Intense atmospheric vortices associated with a 1000 MW fire. *Bull Am Meteorol Soc* 61:682–694
- Clark TL, Jenkins MA, Coen JL, Packham DR (1996a) A coupled atmosphere-fire model: role of the convective Froude number and dynamic fingering at the fireline. *Int J Wildland Fire* 6:177–190
- Clark TL, Jenkins MA, Coen JL, Packham DR (1996b) A coupled atmosphere-fire model: convective feedback on fire-line dynamics. *J Appl Meteorol* 35:875–901
- Clark TL, Coen J, Latham D (2004) Description of a coupled atmosphere-fire model. *Int J Wildland Fire* 13:49–63
- Clarke RH, Dyer AJ, Brook RR, Reid DG, Troup AJ (1971) The Wangara experiment: boundary layer data. Technical paper no 19, CSIRO, Division of Meteorological Physics, Aspendale, 362 pp

- Clements CB (2010) Thermodynamic structure of a grass fire plume. *Int J Wildland Fire* 19:895–902
- Clements CB, Seto D (2015) Observations of fire-atmosphere interactions and near-surface heat transport on a slope. *Bound-Layer Meteorol* 154:409–426
- Clements CB, Zhong S, Goodrick S, Li J, Potter BE, Bian X, Heilman WE, Charney JJ, Perna R, Jang M, Lee D, Patel M, Street S, Aumann G (2007) Observing the dynamics of wildland grass fires. *Bull Am Meteorol Soc* 88:1369–1382
- Clements CB, Zhong S, Bian X, Heilman WE (2008) First observations of turbulence generated by grass fires. *J Geophys Res* 113:D22102. <https://doi.org/10.1029/2008JD010014>
- Clements CB, Davis B, Seto D, Contezac J, Kochanski A, Fillipi J-B, Lareau N, Barboni B, Butler B, Krueger S, Ottmar R, Vihnanek R, Heilman WE, Flynn J, Jenkins MA, Mandel J, Teske C, Jimenez D, O'Brien J, Lefer B (2015) Overview of the 2013 FireFlux-II grass fire field experiment. In: Viegas DX (ed) *Advances in forest fire research*. Coimbra University Press, Coimbra, pp 392–400
- Clements CB, Lareau NP, Seto D, Contezac J, Davis B, Teske C, Zajkowski TJ, Hudak AT, Bright BC, Dickinson MB, Butler BW, Jimenez D, Hiers JK (2016) Fire weather conditions and fire-atmosphere interactions observed during low-intensity prescribed fires – RxCADRE 2012. *Int J Wildland Fire* 25:90–101
- Coen J, Mahalingam S, Daily J (2004) Infrared imagery of crown-fire dynamics during FROSTFIRE. *J Appl Meteorol* 43:1241–1259
- Coen JL, Cameron M, Michalakes J, Patton EG, Riggan PJ, Yedinak KM (2013) WRF-fire: coupled weather-wildland fire modeling with the weather research and forecasting model. *J Appl Meteorol* 52:16–38
- Counihan J (1975) Adiabatic atmospheric boundary layers: a review and analysis of data from the period 1880–1972. *Atmos Environ* 9:871–905
- Crosby JS (1949) Vertical wind currents and fire behavior. *Fire Control Notes* 10:12–15
- Cunningham P, Goodrick SL, Hussaini MY, Linn RR (2005) Coherent vertical structures in numerical simulations of buoyant plumes from wildland fires. *Int J Wildland Fire* 14:61–75
- Deacon EL (1955) Gust variation with height up to 150 m. *Q J R Meteorol Soc* 81:562–573
- Dupuy J-L, Morvan D (2005) Numerical study of a crown fire spreading toward a fuel break using a multiphase physical model. *Int J Wildland Fire* 14:141–151
- Dyer AJ, Hicks BB (1970) Flux-gradient relationships in the constant flux layer. *Q J R Meteorol Soc* 96:715–721
- Emori RI, Saito K (1982) Model experiment of a hazardous forest fire whirl. *Fire Technol* 18:319–327
- Finnigan J (2000) Turbulence in plant canopies. *Ann Rev Fluid Mech* 32:519–571
- Forthofer JM, Goodrick SL (2011) Review of vortices in wildland fire. *J Combust* 2011: Article ID 984363. <https://doi.org/10.1155/2011/984363>
- Gifford F (1957) Relative atmospheric diffusion of smoke puffs. *J Meteorol* 14:410–414
- Goldie AHR (1925) Gustiness of wind in particular cases. *Q J R Meteorol Soc* 51:357–362
- Graham HE (1955) Fire whirlwinds. *Bull Amer Meteorol Soc* 36:99–103
- Haines DA (1982) Horizontal roll vortices and crown fires. *J Appl Meteorol* 21:751–763
- Haines DA (1988) A lower atmospheric severity index for wildland fires. *Nat Weather Dig* 13:23–27
- Haines DA, Smith MC (1983) Wind tunnel generation of horizontal roll vortices over a differentially heated surface. *Nature* 306:351–352
- Haines DA, Smith MC (1987) Three types of horizontal vortices observed in wildland mass and crown fires. *J Clim Appl Meteorol* 26:1624–1637
- Haines DA, Smith MC (1992) Simulation of the collapse of bent-over vortex pairs observed in wildland fires. *For Sci* 38:68–79
- Haugen DA, Kaimal JC, Bradley EF (1971) An experimental study of Reynolds stress and heat flux in the atmospheric surface layer. *Q J R Meteorol Soc* 97:168–180
- Heilman WE (1992) Atmospheric simulations of extreme surface heating episodes on simple hills. *Int J Wildland Fire* 2:99–114
- Heilman WE (1994) Simulations of buoyancy-generated horizontal roll vortices over multiple heating lines. *For Sci* 40:601–617
- Heilman WE, Bian X (2010) Turbulent kinetic energy during wildfires in the north central and northeastern US. *Int J Wildland Fire* 19:346–363
- Heilman WE, Bian X (2013) Climatic variability of near-surface turbulent kinetic energy over the United States: implications for fire-weather predictions. *J Appl Meteorol Climatol* 52:753–771
- Heilman WE, Fast JD (1992) Simulations of horizontal roll vortex development above lines of extreme surface heating. *Int J Wildland Fire* 2:55–68
- Heilman WE, Zhong S, Hom JL, Charney JJ, Kiefer MT, Clark KL, Skowronski N, Bohrer G, Lu W, Liu Y, Kremens R, Bian X, Gallagher M, Patterson M, Nikolic J, Chatziefstratiou T, Stegall C, Forbus K (2013) Development of modeling tools for predicting smoke dispersion from low-intensity fires. Final Report, U.S. Joint Fire Science Program, Project 09-1-04-1. Available: http://www.firescience.gov/projects/09-1-04-1/project/09-1-04-1_final_report.pdf
- Heilman WE, Liu Y, Urbanski S, Kovalev V, Mickler R (2014) Wildland fire emissions, carbon, and climate: plume rise, atmospheric transport, and chemistry processes. *For Ecol Manage* 317:70–79
- Heilman WE, Clements CB, Seto D, Bian X, Clark KL, Skowronski NS, Hom JL (2015) Observations of fire-induced turbulence regimes during low-intensity wildland fires in forested environments: implications for smoke dispersion. *Atmos Sci Lett* 16:453–460
- Heilman WE, Bian X, Clark KL, Skowronski NS, Hom JL, Gallagher MR (2017) Atmospheric turbulence observations in the vicinity of surface fires in forested environments. *J Appl Meteorol Clim* 56:3133–3150

- Hess GD, Hicks BB, Yamada T (1981) The impact of the Wangara experiment. *Bound-Layer Meteorol* 20:135–174
- Hicks BB (1976) Wind-profile relationships from the 'Wangara' experiment. *Q J R Meteorol Soc* 102:535–551
- Hoffman CM, Linn R, Parsons R, Sieg C, Winterkamp J (2015) Modeling spatial and temporal dynamics of wind flow and potential fire behavior following a mountain pine beetle outbreak in a lodgepole pine forest. *Agric For Meteorol* 204:79–93
- Jenkins MA, Clark TL, Coen J (2001) Coupling atmospheric and fire models. In: Johnson EA, Miyanishi K (eds) *Forest fires. Behavior and ecological effects*. Academic, San Diego, pp 257–302
- Kaimal JC, Wyngaard JC, Izumi Y, Coté OR (1972) Spectral characteristics of surface layer turbulence. *Q J R Meteorol Soc* 98:563–589
- Kiefer MT, Zhong S, Heilman WE, Charney JJ, Bian X (2013) Evaluation of an ARPS-based canopy flow modeling system for use in future operational smoke prediction efforts. *J Geophys Res - Atmos* 118:6175–6188
- Kiefer MT, Heilman WE, Zhong S, Charney JJ, Bian X, Skowronski NS, Hom JL, Clark KL, Patterson M, Gallagher MR (2014) Multiscale simulation of a prescribed fire event in the New Jersey pine barrens using ARPS-CANOPY. *J Appl Meteorol Climatol* 53:793–812
- Kiefer MT, Heilman WE, Zhong S, Charney JJ, Bian X (2015) Mean and turbulent flow downstream of a low-intensity fire: influence of canopy and background atmospheric conditions. *J Appl Meteorol Climatol* 54:42–57
- Kiefer MT, Heilman WE, Zhong S, Charney JJ, Bian X (2016) A study of the influence of forest gaps on fire-atmosphere interactions. *Atmos Chem Phys* 16:8499–8509
- Kiefer MT, Zhong S, Heilman WE, Charney JJ, Bian X (2018) A numerical study of atmospheric perturbations induced by heat from a wildland fire: sensitivity to vertical canopy structure and heat source strength. *J Geophys Res - Atmos* 123:2555–2572
- Kolmogorov N (1941) The local structure of turbulence in incompressible fluid for very large Reynolds numbers. *Dokl Akad Nauk SSSR* 30:299
- Koo E, Pagni PJ, Weise DR, Woycheese JP (2010) Firebrands and spotting ignition in large-scale fires. *Int J Wildland Fire* 19:818–843
- Koo E, Linn RR, Pagni PJ, Edminster CB (2012) Modelling firebrand transport in wildfires using HIGRAD/FIRETEC. *Int J Wildland Fire* 21:396–417
- Linn R, Reisner J, Colman JJ, Winterkamp J (2002) Studying wildfire behavior using FIRETEC. *Int J Wildland Fire* 11:233–246
- Liu Y, Goodrick S, Achtemeier G, Jackson WA, Qu JJ, Wang W (2009) Smoke incursions into urban areas: simulation of a Georgia prescribed burn. *Int J Wildland Fire* 18:336–348
- Lumley JL, Panofsky HA (1964) *The structure of atmospheric turbulence*. Interscience, New York, 239 pp
- McRae DJ, Flannigan MD (1990) Development of large vortices on prescribed fires. *Can J For Res* 20:1878–1887
- Mell W, Jenkins MA, Gould J, Cheney P (2007) A physics-based approach to modelling grassland fires. *Int J Wildland Fire* 16:1–22
- Mesinger F, DeMego G, Kalnay E, Mitchell K, Shafran PC, Ebusuzaki W, Jović D, Woollen J, Rogers E, Berbery EH, Ek MB, Fan Y, Grumbine R, Higgins W, Li H, Lin Y, Manikin G, Parrish D, Shi W (2006) North American regional reanalysis. *Bull Am Meteorol Soc* 87:343–360
- Meyers TP, Baldocchi DD (1991) The budgets of turbulent kinetic energy and Reynolds stress within and above a deciduous forest. *Agric For Meteorol* 53:207–222
- Morvan D, Dupuy JL (2004) Modeling the propagation of a wildfire through a Mediterranean shrub using a multiphase formulation. *Combust Flame* 138:199–210
- Mueller E, Mell W, Simeoni A (2014) Large eddy simulation of forest canopy flow for wildland fire modeling. *Can J For Res* 44:1534–1544
- Noble IR, Bary GAV, Gill AM (1980) McArthur's fire-danger meters expressed as equations. *Aust J Ecol* 5:201–203
- Ottmar RD, Hiers JK, Butler BW, Clements CB, Dickinson MB, Hudak AT, O'Brien JJ, Potter BE, Rowell EM, Strand TM, Zajkowski TJ (2016) Measurements, datasets and preliminary results from the RxCADRE project – 2008, 2011 and 2012. *Int J Wildland Fire* 25:1–9
- Panofsky HA, McCormick RA (1954) Properties of the spectrum of atmospheric turbulence at 100 m. *Q J R Meteorol Soc* 80:557–558
- Pimont F, Dupuy J-L, Linn RR, Dupont S (2009) Validation of FIRETEC wind-flows over a canopy and a fuel break. *Int J Wildland Fire* 18:775–790
- Pimont F, Dupuy J-L, Linn RR, Dupont S (2011) Impacts of tree canopy structure on wind flows and fire propagation simulated with FIRETEC. *Ann For Sci* 68:523–530
- Radke LF, Clark TL, Coen JL, Walther CA, Lockwood RN, Riggan PJ, Brass JA, Higgins RG (2000) The wildfire experiment (WiFE): observations with airborne remote sensors. *Can J Remote Sens* 26:406–417
- Raupach MR (1990) Similarity analysis of the interaction of bushfire plumes with ambient winds. *Math Comput Model* 13:113–121
- Raupach MR, Thom AS (1981) Turbulence in and above plant canopies. *Annu Rev Fluid Mech* 13:97–129
- Rawson HER (1913) Atmospheric waves, eddies and vortices. *Aeronaut J* 17:245–256
- Reisner JM, Wynne S, Margolin L, Linn RR (2000) Coupled atmospheric–fire modeling employing the method of averages. *Mon Weather Rev* 128:3683–3691
- Richardson LF (1920) The supply of energy to and from atmospheric eddies. *Proc R Soc A: Math Phys Eng Sci* 97:354–373

- Roth M (2000) Review of atmospheric turbulence over cities. *Q J R Meteorol Soc* 126:941–990
- Rothermel RC (1972) A mathematical model for predicting fire spread in wildland fuels. Research paper INT-115, USDA Forest Service, Intermountain Forest and Range Experiment Station, Ogden
- Seto D, Clements CB (2011) Fire whirl evolution observed during a valley wind-sea breeze reversal. *J Combust* 2011: Article ID 569475. <https://doi.org/10.1155/2011/569475>
- Seto D, Clements CB, Heilman WE (2013) Turbulence spectra measured during fire front passage. *Agric For Meteorol* 169:195–210
- Seto D, Strand TM, Clements CB, Thistle H, Mickler R (2014) Wind and plume thermodynamic structures during low-intensity subcanopy fires. *Agric For Meteorol* 198-199:53–61
- Sharples JJ, McRae RHD, Wilkes SR (2012) Wind-terrain effects on the propagation of wildfires in rugged terrain: fire channelling. *Int J Wildland Fire* 21:282–296
- Shaw WN (1914) Wind gusts and the structure of aerial disturbances. *Aeronaut J* 18:172–203
- Shaw RH, Silversides RH, Thurtell GW (1974) Some observations of turbulence and turbulent transport within and above plant canopies. *Bound-Layer Meteorol* 5:429–449
- Shaw RH, Hartog GD, Neumann HH (1988) Influence of foliar density and thermal stability on profiles of Reynolds stress and turbulence intensity in a deciduous forest. *Bound-Layer Meteorol* 45:391–409
- Simpson CC, Sharples JJ, Evans JP, McCabe MF (2013) Large eddy simulation of atypical wildland fire spread on leeward slopes. *Int J Wildland Fire* 22:599–614
- Simpson CC, Sharples JJ, Evans JP (2016) Sensitivity of atypical lateral fire spread to wind and slope. *Geophys Res Lett* 43:1744–1751
- Skamarock, WC, Klemp, JB, Dudhia, J, Gill, DO, Barker, DM, Wang, W, Powers JG (2005) A description of the advanced research WRF version 2. NCAR Technical Note NCAR/TN-468+STR. National Center for Atmospheric Research, Boulder
- Strand TM, Rorig M, Yedinak K, Seto D, Allwine E, Garcia FA, O’Keefe, P, Checan VC, Mickler R, Clements C, Lamb B (2013) Sub-canopy transport and dispersion of smoke: a unique observation dataset and model evaluation. Final report, U.S. Joint Fire Science Program, Project 09-1-04-2. Available: http://www.firescience.gov/projects/09-1-04-2/project/09-1-04-2_final_report.pdf
- Stull RB (1988) An introduction to boundary layer meteorology. Kluwer Academic Publishers, Dordrecht
- Sullivan AL (2009) Wildland surface fire spread modelling, 1990–2007. 1: physical and quasi-physical models. *Int J Wildland Fire* 18:349–368
- Sun R, Krueger SK, Jenkins MA, Zulauf MA, Charney JJ (2009) The importance of fire-atmosphere coupling and boundary-layer turbulence to wildfire spread. *Int J Wildland Fire* 18:50–60
- Taylor GI (1938) The spectrum of turbulence. *Proc Roy Soc Lond Ser A Math Phys Sci* 164:476–490
- Vickers D, Thomas CK (2013) Some aspects of the turbulence kinetic energy and fluxes above and beneath a tall open pine forest canopy. *Agric For Meteorol* 181: 143–151
- Wilson NR, Shaw RH (1977) A higher-order closure model for canopy flow. *J Appl Meteorol* 16:1197–1205
- Wyngaard JC (1992) Atmospheric turbulence. *Annu Rev Fluid Mech* 24:205–233
- Wyngaard JC, Coté OR (1971) The budgets of turbulent kinetic energy and temperature variance in the atmospheric surface layer. *J Atmos Sci* 28:190–201
- Xue M, Droegemeier KK, Wong V (2000) The advanced regional prediction system (ARPS) – a multi-scale nonhydrostatic atmosphere simulation and prediction model. Part I: model dynamics and verification. *Meteorol Atmos Phys* 75:463–485
- Xue M, Droegemeier KK, Wong V, Shapiro A, Brewster K, Carr F, Weber D, Liu Y, Wang D (2001) The advanced regional prediction system (ARPS) – a multi-scale nonhydrostatic atmosphere simulation and prediction tool. Part II: model physics and applications. *Meteorol Atmos Phys* 76:143–165
- Zulauf MA (2001) Modeling the effects of boundary layer circulations generated by cumulus convection and leads on large-scale surface fluxes. PhD dissertation, University of Utah